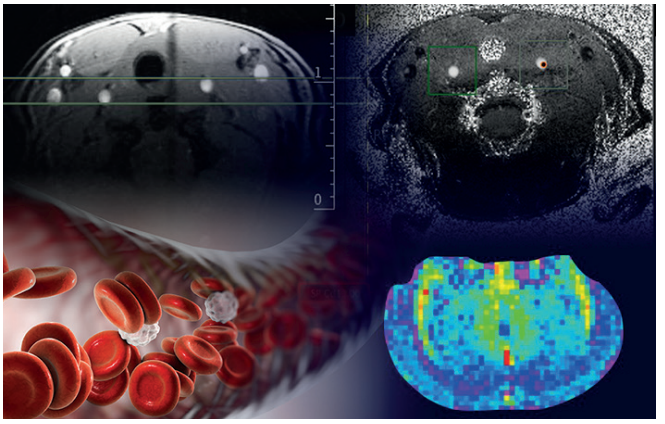

Continuous Arterial Spin Labeling with a Dedicated Labeling Coil

Lydiane Hirschler[1,2#], Clément S. Debacker[1,2#], Jérôme Voiron[2], Sascha Köhler[2], Claire Wary[2], Jan M. Warnking[1], Emmanuel L. Barbier[1]

[1]Univ. Grenoble Alpes, Inserm, Grenoble Institut des Neurosciences, F-38000 Grenoble, France
[2]Bruker Biospin MRI GmbH, 76275 Ettlingen, Germany

[#]co-first authors.

Introduction

Among all existing methods to map cerebral blood flow (CBF), the least invasive is arterial spin labelled (ASL) magnetic resonance imaging (MRI). This technique deposits no ionizing radiation and no tracer injection is required (1). Instead, arterial water is used as an endogenous tracer within an MRI sequence. To use blood as a tracer, the latter can be magnetically labelled. This labeling relaxes with a decay time of only a few seconds, after which the blood magnetization has returned to equilibrium. Taken together with the possibility of absolute CBF quantification and the innocuity of ASL-MRI, this allows measurements to be repeated, providing access to changes in CBF on timescales ranging from seconds to months, an attractive characteristic for pharmacological MRI.

Labeling can be achieved through various techniques that can be divided in three main categories: pulsed ASL (PASL), continuous ASL (CASL) and velocity-selective ASL (vsASL). The details of these techniques have been reviewed by several authors (2,3).

Even though the ASL development originally started in animals with CASL (4), subsequent development has mainly been performed in humans. As a result, clinically available ASL methods are today far more mature than those for preclinical use (Table 1) (5). Given the numerous animal models used in the field of neuroscience and the important role of MRI in brain research, there is a need to make preclinical ASL more robust. In this study, we evaluate the use of CASL with a separate labeling RF coil and pseudo-continuous ASL (pCASL), which has become the recommended technique for clinical studies (6). At 7.0 T, we compare CBF values obtained using both approaches and at 9.4 T, we compare specific absorption rate (SAR).

		Clinical ASL	Preclinical ASL
Main ASL schemes	PASL	4	3
	CASL with volume coil	2	3
	CASL with labeling coil	1	3
	Unbalanced pCASL	4	1
	Balanced pCASL	4	1
	vsASL	3	0
Advanced features	Time-encoded ASL	2	1
	Perfusion territory map	2	0
	3D readout	4	1
	Background suppression	4	1

Table 1. Maturity of ASL methods in clinical and preclinical settings. 0: never tested, 1: concept demonstration, 2: common in research use, 3: commercially available, 4: mature technology.

Materials and methods

Animals and experiments

Male rats (Wistar at 7.0 T or Sprague Dawley at 9.4 T, Charles River, France) were used. All experiments were approved by the local ethics committee and were performed in full compliance with the guidelines of the European community (EUVD 86/609/EEC) for the care and use of the laboratory animals. Experiments were performed under permits n°380945 for EBand A3851610008 for experimental and animal care facilities from the French Ministry of Agriculture. All procedures were performed under isoflurane anaesthesia (IsoFlo, Axience, France, 5% for induction, 2% for maintenance). Respiration rate, heart rate and oxygen saturation were monitored and maintained within the following ranges: 40-60 breaths per minute, 400-500 beats per minute and 98-100%, respectively. Hot water was circulated inside the cradle under the animal's body to prevent hypothermia under anaesthesia. Note that head and the neck were located outside of the heated area of the cradle to prevent water from circulating through the labeling and imaging volumes of interest.
At 7.0 T, multi-slice CASL and pCASL images were acquired in the same animals (n=9, 384±21 g) to compare the CBF values. At 9.4 T, the SAR was monitored in animals equipped with fiber-optic temperature probes (cf. below) using singleslice CASL and pCASL (n=9, 231±29 g).

Figure 1: ASL Labeling coil in the cradle.

Temperature monitoring

To measure the heating induced by the MR scans performed at 9.4 T, local tissue temperature was continuously measured in nine animals using fiber-optic temperature probes (model FTP-LTF2-ST-10M, Photon Control, Burnaby, BC, Canada; diameter: 650 µm; sampling frequency of 10 Hz). The temperature probes with a ~200µm sensitive tip were implanted at two different locations: (i) within the brain and (ii) subcutaneously near the labeling plane (between carotids). The position of the two probes varied across animals. Different brain areas were sampled for different animals, across striatum and cortex.

MRI

Experiments were performed on both a 7.0 T (Bruker Biospec, AVANCE III) and a 9.4 T (Bruker Biospec, AVANCE III HD) horizontal bore preclinical scanners using 3 types of Bruker RF coils:

- a transmit-receive volume coil (72 mm inner diameter at 7.0 T and 86 mm inner diameter at 9.4 T) for imaging and labeling,
- a receive-only surface rat head coil (single channel at 7.0 T; phased-array, 4-channel at 9.4 T) for imaging,
- a transmit-receive, single-loop ASL coil (diameter 23 x 21 mm^2) placed under the animal's throat for labeling (Fig. 1). The position of the coil was manually adjusted in the head-foot direction.

The following sequences were performed. Unless mentioned otherwise, sequences were performed at both 7.0 and 9.4 T:

- Standard adjustments: volume coil tuning and matching, basic frequency adjustment, standard global first order shim, volume coil RF pulse power calibration and B_1 maps to adjust the ASL coil reference power;
- At 9.4 T, FLASH scans to visualize the fiber-optic probe's position in the carotids (TR/TE = 120/1.6 ms, resolution 0.195x0.195x0.8 mm^3, number of averages (NA) = 2, acquisition time Tacq = 31 s, 20 slices);
- Anatomical axial T_2-weighted (T_2w) images acquired through a spin-echo T2-TurboRARE sequence (at 7.0 T: Rare factor 8, TR/TE=3728/31 ms, resolution 0.125x0.125x0.8 mm^3, NA = 2, Tacq = 3 min 58 s, 35 slices; at 9.4 T: RARE factor 8, TR/TE = 3139/33 ms, resolution 0.137x0.137x0.8 mm^3, NA = 2, Tacq = 3 min 21 s, 30 slices);
- At 7.0 T, Inversion Efficiency (IE) was measured 5 mm downstream of the labeling plane with a flowcompensated, ASL-encoded FLASH (FcFLASH) sequence for each ASL labeling scheme.
- At 7.0 T, a T_1 map using a non-selective inversion recovery (IR), spin-echo EPI, sequence (TR/TE=10000/20 ms, adiabatic inversion pulse, 18 inversion times between 35 and 10000 ms, NA=1, Tacq=4 min) (7);
- CASL-EPI sequences using the ASL coil for labeling;
- pCASL-EPI sequences using the volume RF coil for labeling.

All labeling pulses targeted a slice in the neck (at 2 cm from the isocenter) during τ= 3 s followed by a post-labeling delay (ω) (200 ms at 7.0 T; 300 ms at 9.4 T). The acquisition was single-shot spin-echo echo-planar imaging (EPI) (at 7.0 T, TR/TE= 22/3500 ms, 0.25x0.25x0.8mm^3, 5 slices for multislice experiments; at 9.4 T, TR/TE= 22/4000 ms, in-plane resolution 0.234x0.234x1 mm^3, 1 slice for temperature measurements), performed with the volume coil as transmit and the surface array coil as receive. Thirty pairs of label/ control images were acquired within 4 minutes. Labeling pulse-trains for pCASL consisted of 400-µs Hanning window shaped RF pulses repeated every 800 µs. The maximum and the mean values of the pCASL labeling gradient were 45 and 5 mT/m, respectively. The CASL gradient was 10 mT/m. The inter-pulse phase increments of pCASL were optimized as described in (8). The average labeling B_1 of each ASL scheme was 3.1 µT at 7.0 T and 5 µT at 9.4 T.

CASL and pCASL processing

MRI data were analyzed using software developed in-house in Matlab (The MathWorks Inc., Natick, MA). T_1 maps were obtained by fitting the following equation to the signal from each pixel using a Levenberg-Marquardt algorithm:

$$M_z(TI) = M_0 \cdot \left(1 - 2\kappa e^{-TI/T_1}\right), \quad [1]$$

where $M_z(TI)$ is the MR signal collected at each inversion time TI, M_0 the magnetization at thermal equilibrium, T_1 the longitudinal relaxation time constant of tissue and k the inversion efficiency.

The label inversion efficiency IE was derived from a complex reconstruction of the (p) CASL-FcFLASH sequence as follows:

$$IE = \left|\frac{M_C - M_L}{2M_C}\right|, \quad [2]$$

where M_C and M_L are respectively the complex signals from the control and the label experiments. A region of interest (ROI) was manually drawn on each carotid. IE was obtained as the mean IE across both carotids.

To calculate quantitative CBF maps, we assumed a single compartment and used the standard kinetic model developed by Buxton et al. (9). Assuming that the arterial transit time is equal to the post-labeling delay and that M_0^b, the magnetization of arterial blood at thermal equilibrium, may be approximated by M_0^t/λ, where M_0^t is the magnetization of tissue at thermal equilibrium and the λ blood-brain partition coefficient of water (0.9 mL/g (2)), we used the following equation pixel-by-pixel to quantify CBF (mL/100 g/ min) (1,3,4):

$$CBF = \frac{\lambda \cdot \Delta M \cdot exp\left(\omega/T_1^b\right)}{2IE \cdot T_1^t \cdot M_0^t \cdot \left(1 - exp\left(-\tau/T_1^t\right)\right)}, \quad [3]$$

where ΔM is the signal difference between control and label acquisitions averaged over repetitions; T_1^t is the apparent T_1 of tissue from the T_1 map; T_1^b is the longitudinal relaxation time of blood (2.304 s at 7.0 T (10)). M_0^t is the control image intensity of the ASL experiment multiplied by $[1 - exp(-TR/T_1^t)]^{-1}$ to correct for incomplete longitudinal relaxation during the 4-s TR.

Temperature processing

The animal body temperature was maintained by intermittent heating periods, leading to slow fluctuation of animal temperature over the course of the experiment. To avoid confounding effects on SAR measurements, a linear temperature drift was obtained from a 3-min baseline immediately prior to each MRI acquisition and removed from the subsequent data. Then, 45 s after onset of the MRI scan, a linear curve was fitted to the next 1.5 minutes of the temperature increase and the apparent SAR (SAR_{app}) was calculated with:

$$SAR_{app} = S_{scan} \cdot C_{tissue}, \quad [4]$$

where S_{scan} is the fitted slope of the temperature increase and C_{tissue} the specific heat capacity of tissue (3664 J·(kg·K)$^{-1}$ (11)).

Results

At 7.0 T, the IE of CASL (85.2±1.5%) and pCASL (83.9±1.6%) were similar. Figure 3 shows an example of maps collected in one animal. Brain structures, such as the corpus callosum, are equally well delineated with both the pCASL and the CASL sequences. High intensity pixels due to intra-vascular signal within the brain may also be observed with both sequences. The difference maps show mostly noise. Neither brain structures nor vascular structures may be observed.

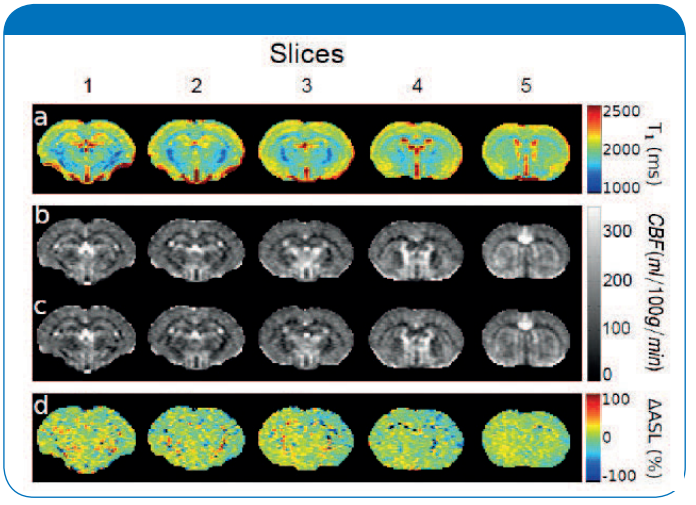

Figure 2: a) T1 map, b) CBF maps obtained with a CASL sequence and a separate labeling coil, c) CBF maps obtained with a pCASL sequence, d) the relative difference between the two CBF maps ((pCASL-CASL)/CASL). Data obtained on the same animal at 7 T.

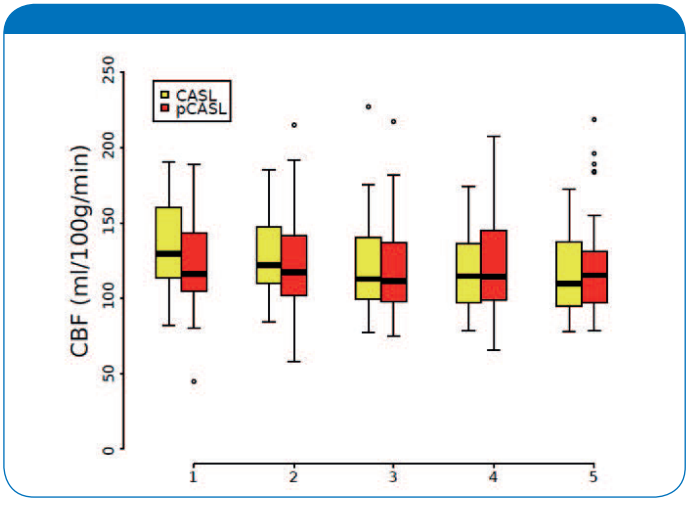

Figure 3: Whisker plot of CBF values obtained with a CASL sequence (separate labeling coil) and a pCASL sequence on 9 rats. IE was measured animal per animal. The pCASL and the CASL sequences were performed in the same animals at 7 T (n=9). Black lines indicate median values. Boxes represent the range from the first to third quartile of the measured values. Data points are labeled as outliers, if their distance to the box is larger than 1.5 times the size of the box. Whiskers indicate the range of data points that are not considered outliers.

From a statistical point of view, no difference was observed between the two methods. The CBF values measured with CASL and pCASL (109.6±17.5 and 109.1±15.7 ml/100g/min, respectively) were not different. Figure 3 shows the distribution of CBF values for each slice and each ASL sequence. The two sequences yielded CBF values within the same intervals.

CASL and pCASL: Temperature

Figure 5 shows an example of the temperature time courses corrected for drift in one animal. The temperature is stable prior to the sequence onset and rises almost linearly until the end of the sequence. At both measurement locations, the temperature during the pCASL remains comparable to that of the T2W sequence, while that measured during the CASL with labeling coil is lower.

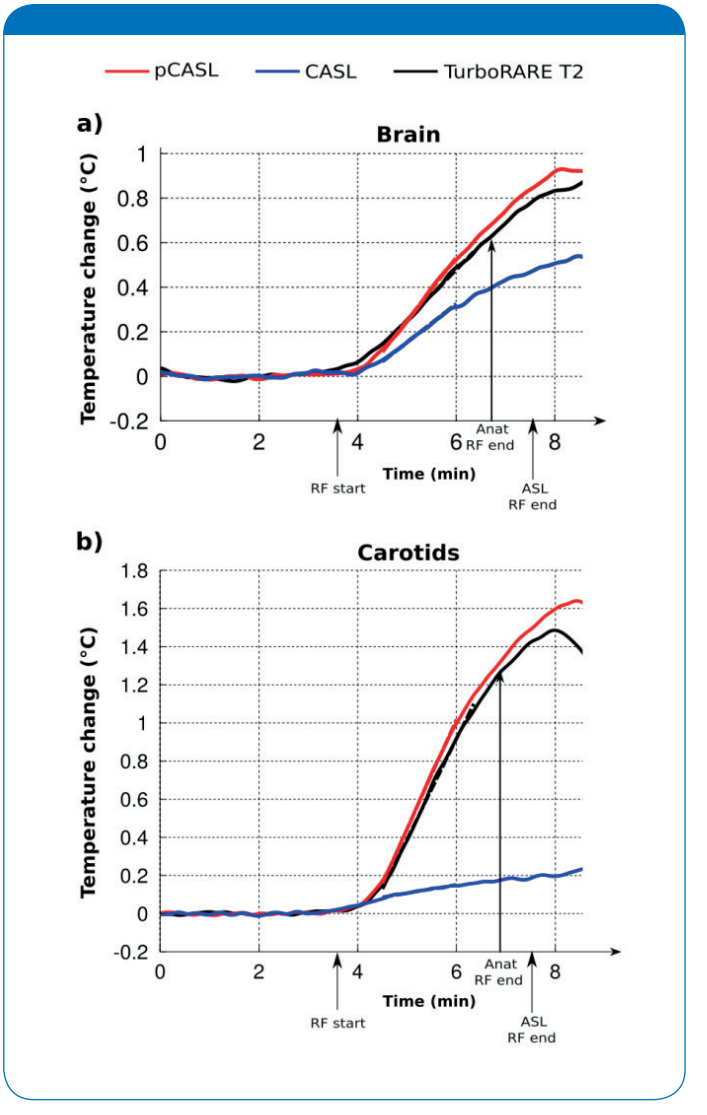

Figure 4: Exemplary temperature time courses measured in a) the brain and b) in the neck between the carotids of one animal, during pCASL (red), turbo-RARE T_2w (black), and CASL (blue) sequences after drift correction. For the sake of clarity, the three temperature time courses were aligned at onset of sequence (denoted by the RF start arrow). The end of the anatomical T_2w sequence is indicated by the "Anat RF end" arrow and that of the two ASL scans by the "ASL RF end" arrow.

Global temperature increase in TurboRare and ASL sequences

The observed temperature increase did not result only from the RF irradiation. By applying the ASL sequences with RF pulses of zero amplitude we observed an increase in temperature due to heating of the receiver coil decoupling circuit (data not shown). Both pCASL and CASL are particularly affected due to the long labeling duration, during which the decoupling circuit of the receiver coil is active. Thus, with our current coils and experimental setup, the global apparent SAR in the brain resulting from the combination of decoupling and RF effects was 19.7±18.1 W/kg for the pCASL and 11.1±12.6 W/kg for the CASL with a labeling coil. In comparison, the RF-intensive 30-slice TurboRARE anatomical imaging sequence used in this study exhibited a global apparent SAR of 13.0±8.5 W/kg in the brain. The large variability of these values can be attributed to the variable positioning of the temperature probes between animals.

Temperature increase in ASL sequences due to RF irradiation.

For the ASL sequences, acquisitions were performed with RF=0, and for several ASL-B_1 values in order to decompose the global SAR into heating from the labeling RF itself and that from the active decoupling (12). With a prescribed B_1 of 5 µT during the labeling period and in single slice mode, the $B1_{rms}$ over the duration of the entire sequence was numerically estimated at 3.1 µT for CASL and 7.5 µT for pCASL. The peak B1 values are higher in the pCASL sequence than in the CASL sequence due to the pulsed nature of the RF in the former. After correcting individual temperature time courses for the contribution due to the decoupling circuit, the average calculated SAR originating from the RF were 11.1±7.1 W/kg and -0.1±1.0 W/kg for pCASL and CASL respectively in the brain and 13.3±5.4 W/kg and 1.8±1.2 W/kg for pCASL and CASL at the carotid level of all animals. Using Eq. [4], these SAR values were converted to temperature increases. For pCASL, the labeling RF produced an increase of 0.73±0.47°C in brain temperature and 0.87±0.35°C near the carotids after a 4-min scan. For CASL with labeling coil, one calculates that there should be no temperature increase owing to RF-heating in the brain, and a 0.12±0.08°C increase near the carotids after a 4-min scan.

Discussion and conclusion

In this study, we compared the performance of two approaches for measuring tissue perfusion by MRI: pCASL, the consensus sequence for human use, and CASL with a dedicated labeling coil. Importantly, the two modalities used here are free from Magnetization Transfer (MT) effects – pCASL intrinsically because of the short-pulse labeling scheme, and CASL because it was performed here with a dedicated labeling coil. Hence, they both allow multi-slice acquisitions, and with the IE calculation, both provide absolute measurements of perfusion. In terms of quantification, both sequences yielded comparable CBF maps and values with the same sensitivity and precision.

As expected, the SAR evaluation performed at 9.4 T demonstrated that CASL operated with a dedicated labeling coil delivered a much lower SAR than pCASL.

Under the present conditions, the SAR owing to RF itself produced an average increase in brain temperature of less than 1°C with pCASL, while RF heating owing to CASL operated with a labeling coil was negligible in the brain. Since SAR issues worsen as the magnetic field increases, this result is in favor of using a dedicated labeling coil at higher magnetic fields, where temperature rises may exceed 1°C, or for very long scans where continuous monitoring of CBF with ASL is required. Nonetheless, with the current coils, we also found a contribution from heating owing to the receiver coil decoupling circuit, which requires further investigation and are further detailed in (12).

Independently of SAR issues, it has also been shown that pCASL is sensitive to B_0 heterogeneity in the labeling area and requires specific corrections at high magnetic field, while CASL is not sensitive to this issue (8). Thus, both sequences can equally well map CBF in small animals and optimal choice of sequences to map CBF will depend on experimental design and field strength.

An important factor in conducting ASL experiments and obtaining reliable CBF measurements from them is operating the necessary pre-scans and calibration steps specific to each sequence. The extra time required to install and calibrate the labeling coil for CASL may be regained by removing the calibrations steps specifically required for pCASL (8). More importantly still, the workflow of adjustments and corrections itemized above in Materials and Methods should be streamlined, made robust, and automated as much as possible.

One objective of the present collaboration between Bruker Biospin MRI and Grenoble Institute of Neuroscience (GIN) was therefore to introduce software tools which integrated all individual steps specifically for the CASL experiment. Annex 1 highlights the new developments which are incorporated into the next release of ParaVision. An exemplary workflow for the CASL setup using the Labeling Coil is illustrated in Annex 2 and includes:

- Auto setting of labeling power from coil power adjustment
- Inversion Efficiency measurement including automated vessel recognition
- CASL-EPI reconstruction with either native images, relative or quantitative perfusion maps using the calculated IE

Altogether, introducing advanced correction features for ASL methods within a simplified workflow including pre-configured scan programs will help ASL methods gain maturity in preclinical settings, and help improve accuracy and reproductibility in preclinical perfusion quantification.

Annex: Methods and Protocols for facilitated workflow

Annex 1: New developments

- The CASL_FcFLASH method was developed to measure the Labeling Inversion Efficiency (IE). It includes automated carotid delineation and IE calculation. Furthermore, to aid the user and facilitate the experiment, a guide card summarizing the workflow was integrated into the CASL_FcFLASH method (Fig. A.1).

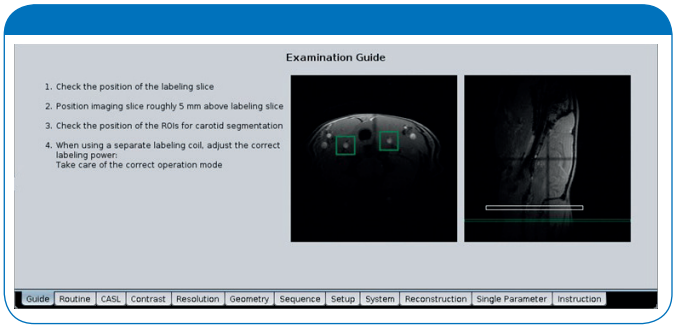

Figure A.1: CASL_workflow guide

- The CASL_EPI method has been adapted to directly produce CBF maps, whether relative (%) or absolute (ml/min/100gtissue), according to eq.[3]. Additionally, it can be parametrized to exclude outliers in repeated measurements (Fig. A.2) based on the method of Tan et al. (13).

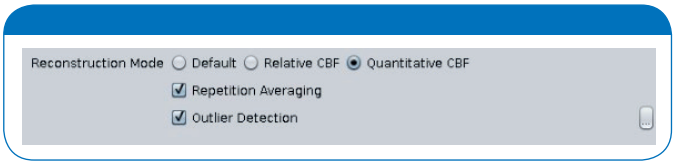

Figure A.2: Reconstruction options of the CASL_EPI method

- By default, the quantitative CBF map will automaticallyuse the measured IE measured with CASL_FcFLASH if it exists. Alternatively, the IE can also be set to a defined value (Fig A.3).

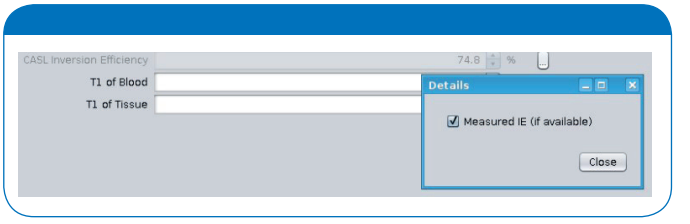

Figure A.3: option for the IE

- An optimization of the control frequency to improve MT correction when using the CASL without a dedicated labeling coil is included in the adjustment platform of the CASL_EPI and can be run on demand prior to the acquisition (Fig A.4).

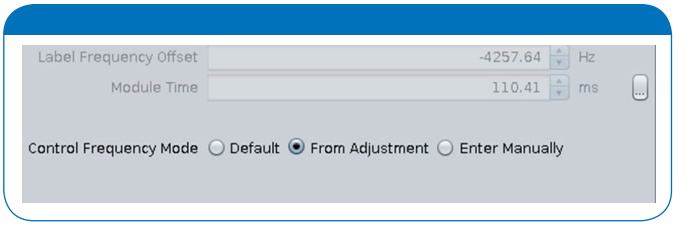

Figure A.4: Control Frequency Mode

- The Labeling power is automatically calculated from RF calibration or the user specified B1, both for CASL_FcFlash and for CASL_EPI sequences (Fig A.5).

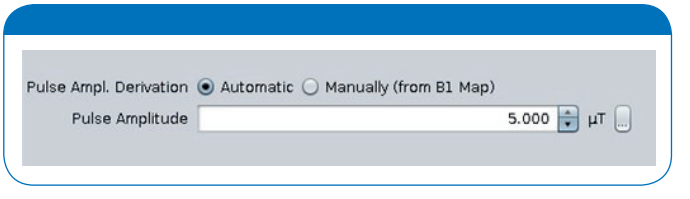

Figure A.5: Pulse Amplitude Derivation setting

The improved methods, including dedicated adjustments and reconstruction tools are available in ParaVision versions 7 and 360 at all fields.

Annex 2: Exemplary workflow for CASL with a Labeling Coil

Pre-optimized protocols have been designed for use on rat animal models with a dedicated surface ASL coil for labeling of the carotids with limited SAR deposition. They are grouped together as a Scan Program CASL_Perfusion_with_Labeling_Coil to enable a streamlined workflow (Fig A.6).

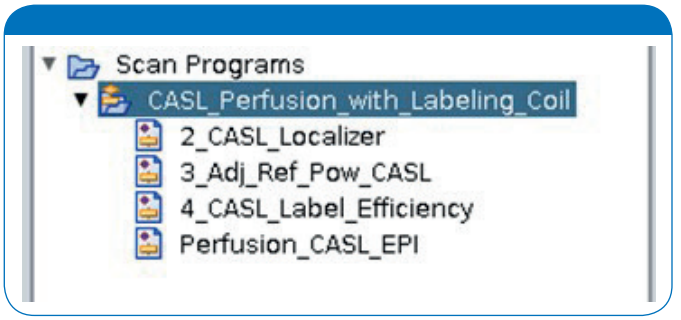

Figure A.6: Example of Scan Program for CASL CBF measurement with a Labeling Coil

- First, to localize the carotids, the 2_CASL_Localizer is run with the volume coil as transmitter and the CASL coil as receiver. It acquires multislice flow compensated images to enable precise separation of the common carotid into external and internal carotids (Fig A.7a).

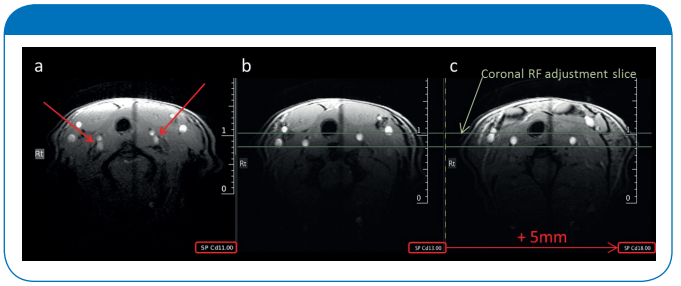

Figure A.7: Output from 2_CASL_Localizer and planning for 3_Adj_Ref_Pow_CASL a. Carotid Split. b. Slice for imaging IE c. Labeling Slice

The slice for measuring the IE (Fig A.7b), is selected 1 or 2 mm upstream from the separation of the carotids, and the labeling slice is placed 5 mm further upstream (Fig A.7c)

- In a second step, 3_Adj_Ref_Power_CASL is used to calibrate the reference power. The CASL coil is set to Transmit/ Receive mode and the reference power is adjusted in a coronal plane covering the carotids which is placed in the slice selected for labeling (Fig A.7c).

- In the 4_CASL_Label_Efficiency step, predefined geometrical objects appear in the slice selected to measure the IE and must be placed over the carotids by simple drag and drop operation (Fig A.8a).

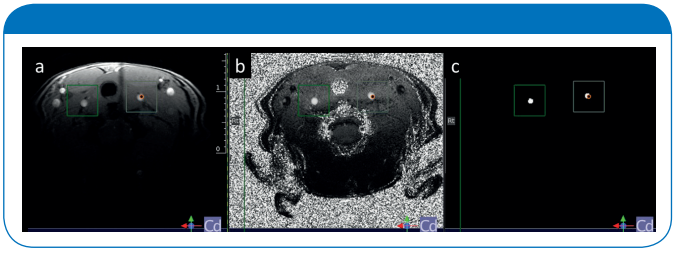

Figure A.8: CASL_Label_Efficiency: a. Positioning of geometrical objects over the carotids b. Resulting IE map c. Pixels used for IE calculation

The sequence automatically generates two frames: The IE map (Fig A.8b) and a frame containing only the pixels used to calculate the IE from the two automatically delineated carotids (Fig A8c). The average of IE calculated in the two carotids (IE Mean) is automatically carried over to the CASL_EPI sequence for CBF calculation.

- In the final step, Perfusion_CASL_EPI is run to generate the perfusion maps. The perfusion scan, typically run with 30-40 repetitions, will automatically integrate previous calibrations to generate a quantitative perfusion map. The derived perfusion map may then simply be displayed in the viewing card (Fig A.10).

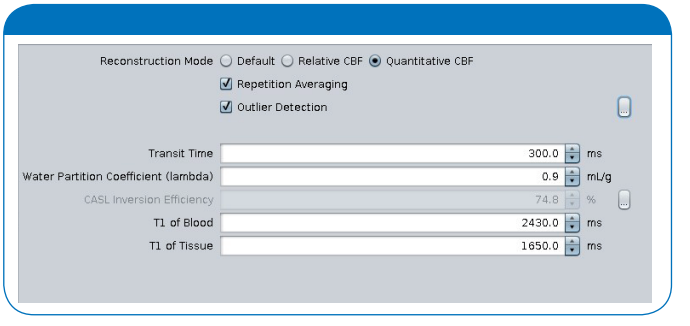

Figure A.9: Reconstruction parameters for automatic CBF map calculation.

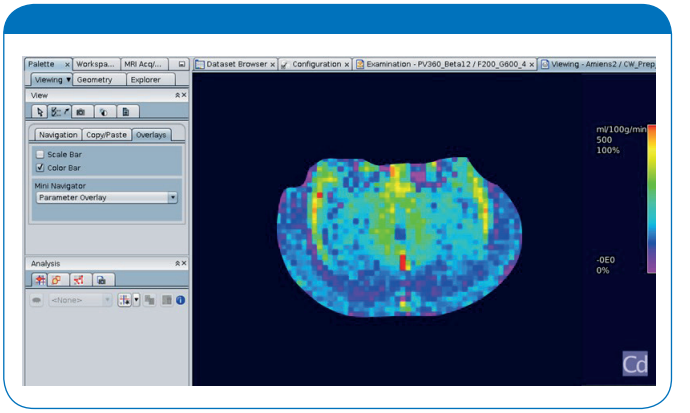

Figure A.10: Perfusion_CASL_EPI: quantitative perfusion map (CBF) acquired in 6 min at 7T in healthy rat brain

References

[1] Wintermark M, Sesay M, Barbier E, Borbely K, Dillon WP, Eastwood JD, Glenn TC, Grandin CB, Pedraza S, Soustiel JF, Nariai T, Zaharchuk G, Caille JM, Dousset V, Yonas H. Comparative overview of brain perfusion imaging techniques. Stroke 2005;36(9):e83-e99.

[2] Barbier EL, Lamalle L, Decorps M. Methodology of brain perfusion imaging. J Magn Reson Imaging 2001;13(4):496-520.

[3] Calamante F, Thomas DL, Pell GS, Wiersma J, Turner R. Measuring cerebral blood flow using magnetic resonance imaging techniques. Journal of Cerebral Blood Flow and Metabolism 1999;19:701-735.

[4] Detre JA, Leigh JS, Williams DS, Koretsky AP. Perfusion imaging. Magnetic Resonance in Medicine 1992;23(1):37-45.

[5] Hernandez-Garcia L, Lahiri A, Schollenberger J. Recent progress in ASL. Neuroimage 2018.

[6] Alsop DC, Detre JA, Golay X, Gunther M, Hendrikse J, Hernandez-Garcia L, Lu H, MacIntosh BJ, Parkes LM, Smits M, van Osch MJ, Wang DJ, Wong EC, Zaharchuk G. Recommended implementation of arterial spin-labeled perfusion MRI for clinical applications: A consensus of the ISMRM perfusion study group and the European consortium for ASL in dementia. Magnetic resonance in medicine : official journal of the Society of Magnetic Resonance in Medicine / Society of Magnetic Resonance in Medicine 2015;73(1):102-116.

[7] Debacker CS, Daoust A, Kohler S, Voiron J, Warnking JM, Barbier EL. Impact of tissue T_1 on perfusion measurement with arterial spin labeling. Magnetic resonance in medicine : official journal of the Society of Magnetic Resonance in Medicine / Society of Magnetic Resonance in Medicine 2017;77(4):1656-1664.

[8] Hirschler L, Debacker CS, Voiron J, Kohler S, Warnking JM, Barbier EL. Interpulse phase corrections for unbalanced pseudo-continuous arterial spin labeling at high magnetic field. Magnetic resonance in medicine : official journal of the Society of Magnetic Resonance in Medicine / Society of Magnetic Resonance in Medicine 2018;79(3):1314-1324.

[9] Buxton R. B., Frank, L. R., Wong, E. C., Siewert, B., Warach, S., Edelman, R. R., 1998. A general kinetic model for quantitative perfusion imaging with arterial spin labeling. Magn. Reson. Med. 40 (3), 383–396

[10] Barbier EL, St Lawrence KS, Grillon E, Koretsky AP, Decorps M. A model of blood-brain barrier permeability to water: accounting for blood inflow and longitudinal relaxationeffects. Magn. Reson. Med 2002;47(6):1100-1109.

[11] Sotero RC, Iturria-Medina Y. From blood oxygenation level dependent (BOLD) signals to brain temperature maps. Bull Math Biol 2011;73(11):2731-2747.

[12] Hirschler L, Collomb N, Voiron J, Köhler S, Barbier EL, Warnking JM. SAR comparison between CASL and pCASL at high magnetic field and evaluation of the benefit of a dedicated labeling coil. Magn Reson Med. 2020 Jan;83(1):254-261.

[13] Tan, H., Maldjian, J. A., Pollock, J. M., Burdette, J. H., Yang, L. Y., Deibler, A. R., Kraft, R. A. A fast, effective filtering method for improving clinic

Bruker BioSpin

info@bruker.com
www.bruker.com